

Supporting Information for
**Redox Behavior and Dioxygen Reactivity of a Macrocyclic Carboxylate-Bridged
Diiron(II) Mimic of Bacterial Monooxygenase Active Sites**

*Loi H. Do, Stephen J. Lippard**

Department of Chemistry, Massachusetts Institute of Technology, Cambridge, MA 02139.

<u>Contents</u>	<u>Page(s)</u>
Experimental	S2-S5
Spectroscopic and Electrochemical Data	S6-S17
Figure S1. Titration plots of PIM ²⁻ with Fe(II) and carboxylates.	S6
Figure S2. ¹ H NMR spectrum of [Fe ₂ (PIM)(Ph ₃ CCO ₂) ₂] (1).	S7
Figure S3. EPR Spectrum of 1 .	S8
Figure S4. Cyclic voltammograms of 1 and 2 .	S9
Figure S5. Absorption spectrum of 3 .	S10
Figure S6. Absorption spectrum of 2 + AgSbF ₆ .	S11
Figure S7. Zero-field Mössbauer spectrum of ⁵⁷ Fe enriched 3 .	S12
Figure S8. Zero-field Mössbauer spectrum of ⁵⁷ Fe enriched 1 + O ₂ .	S13
Figure S9. Zero-field Mössbauer spectrum of ⁵⁷ Fe enriched 4 and 5 .	S14
Figure S10. ¹ H NMR Spectrum of 2 + O ₂ .	S15
Figure S11. UV-vis spectrum of 2 /O ₂ and 2 /O ₂ + H ₂ O	S16
Figure S12. Solution Mössbauer spectrum of 2 , 6/7 , and 8	S17
Crystallographic Data and Analysis	S18-S28
X-ray Crystallographic Refinement	S18-S19
Figure S13. X-ray structure of 1 showing 50% thermal ellipsoids.	S20
Figure S14. X-ray structure of 2 showing 35% thermal ellipsoids.	S21
Figure S15. X-ray structure of 3 showing 50% thermal ellipsoids.	S22
Figure S16. X-ray structure of 4 showing 50% thermal ellipsoids.	S23
Figure S17. X-ray structure of 5 showing 50% thermal ellipsoids.	S24
Figure S18. X-ray structure of 6/7 showing 35% thermal ellipsoids.	S25
Table S1. X-ray data collection and refinement parameters for 1-7 .	S26-S27
Table S2. Bond valence sum analysis of 3 , 6 , and 7 .	S28
References	S29

EXPERIMENTAL

Materials and Methods. Reagents obtained from Strem, Aldrich Chemical Co., and Alfa Aesar were used as received. The compound 2-(2-bromo-4-methylphenoxy)-tetrahydro-2H-pyran was prepared as described.¹ All air-sensitive manipulations were performed using standard Schlenk techniques or under a nitrogen atmosphere inside an MBraun drybox. Solvents were saturated with argon and purified by passage through two columns of activated alumina.

3,3'-[Oxybis(methylene)]bis(bromobenzene) (A). 3-Bromobenzylalcohol (3.72 g, 20 mmol) was dissolved in 50 mL of dry THF and cooled to 0 °C with an ice bath. Solid sodium hydride, 0.96 g, 24 mmol, 60% dispersion in mineral oil, was added portionwise to the reaction flask and the mixture was stirred for 1 h. Liquid 3-bromobenzylbromide (5.0 g, 20 mmol) was then added and the solution was stirred at reflux for 12 h. Water was slowly added to quench the reaction and the organic phase was extracted into diethyl ether, dried over Na₂SO₄, filtered, and evaporated to yield a light yellow oil (7.12 g, 99%). This material was determined to be > 98% pure by NMR spectroscopy and gas chromatography. ¹H NMR (CDCl₃, 500 MHz): δ 7.56 (s, 2H), 7.46 (d, *J* = 9.0 Hz, 2H), 7.31 (d, *J* = 7.5 Hz, 2H), 7.25 (t, *J* = 8.0 Hz, 2H), 4.53 (s, 4H) ppm. ¹³C NMR (CDCl₃, 125 MHz): δ 140.38, 130.82, 130.62, 130.16, 126.18, 122.64, 71.82 ppm. GC-MS = 356 [M]⁺ (Calcd = 355.9 [M]⁺).

2,2'-[(Oxybis(methylene))bis(5-methyl-[1,1'-biphenyl]-3',2-diyl)]bis(oxy)bis(tetrahydro-2H-pyran) (B). 2-(2-Bromo-4-methylphenoxy)-tetrahydro-2H-pyran¹ (16.5 g, 61.1 mmol) was dissolved in 250 mL of dry THF and cooled to -78 °C. The solution was treated with *n*-butyllithium (38 mL, 1.6 M in hexanes) and stirred for 2 h, giving a white slurry. A 50 mL solution of zinc chloride (6.66 g, 61.1 mmol) in THF was transferred by cannula to the reaction flask. After 1 h, the solution became nearly homogeneous. The reaction flask was charged with compound A (10.0 g, 28.1 mmol) and Pd(PPh₃)₄ (3.25 g, 2.81 mmol) and refluxed for 2 d. Once the reaction was complete, the

solution was evaporated to dryness and the crude material was purified by silica gel column chromatography (5% ethyl acetate/ 95% hexanes) to afford a colorless oil (5.7 g, 35%). ¹H NMR (CDCl₃, 500 MHz): δ 7.67 (s, 2H), 7.58 (d, *J* = 8.0 Hz, 2H), 7.45 (t, *J* = 7.5 Hz, 2H), 7.40 (d, *J* = 7.5 Hz, 2H), 7.24 (s, 2H), 7.20 (d, *J* = 8.5 Hz, 2H), 7.15 (d, *J* = 8.5 Hz, 2H), 5.42 (t, *J* = 2.5 Hz, 2H), 4.71 (s, 4H), 3.84 (m, 2H), 3.59 (m, 2H), 2.39 (s, 6H), 1.89 (m, 2H), 1.76 (m, 4H), 1.67 (m, 2H), 1.54 (m, 4H) ppm. ¹³C NMR (CDCl₃, 125 MHz): δ 151.80, 138.95, 137.85, 131.46, 131.30, 131.28, 129.22, 129.09, 129.00, 127.93, 126.28, 116.12, 96.89, 72.44, 61.76, 30.35, 25.34, 20.70, 18.54 ppm.

Bis(3-(2-hydroxy-5-methylphenyl)benzyl)ether (C). Compound **B** (0.90 g, 1.56 mmol) and oxalic acid (0.35 g, 3.89 mmol) were dissolved in 10 mL of THF/MeOH (1:1). The mixture was stirred at ~50 °C for 2 h and then evaporated to dryness. Dichloromethane (10 mL) was added and the mixture was washed with water (3 x 10 mL). The organic layer was dried over Na₂SO₄, filtered, and the solvent was removed in vacuo to give an off-white solid. The solid was washed with hot hexanes to remove a colored impurity and the final product was isolated by filtration (0.46 g, 73%). ¹H NMR (CDCl₃, 500 MHz): δ 7.54 (s, 2H), 7.48 (d, *J* = 7.5 Hz, 2H), 7.43 (m, 4H), 7.09 (m, 4H), 6.87 (d, *J* = 8.0 Hz, 2H), 5.43 (s, 2H), 4.67 (s, 4H), 2.35 (s, 6H) ppm. ¹³C NMR (CDCl₃, 125 MHz): δ 151.00, 139.68, 138.43, 131.54, 130.70, 130.33, 129.93, 129.38, 129.21, 128.50, 127.86, 116.56, 73.02, 21.26 ppm. ESI-MS(-) = 409.1 [M-H]⁻ (Calcd = 409.2 [M-H]⁻). Mp = 128-130 °C.

Bis(3-(2-hydroxy-5-methylphenyl-3-carbaldehyde)benzyl)ether (D). This reaction is water sensitive so it is important that all reagents and solvents are rigorously dried. Compound **C** (2.44 g, 5.95 mmol), anhydrous magnesium chloride (2.26 g, 23.8 mmol), paraformaldehyde (2.68 g, 89.2 mmol), and triethylamine (5 mL, 35.7 mmol) were combined in 200 mL of dry acetonitrile and refluxed for 3 d. The reaction completeness was determined by the disappearance of starting material

using silica thin layer chromatography. The mixture was evaporated to dryness and the residue was dissolved in dichloromethane. The organic phase was washed with aqueous HCl, dried over Na₂SO₄, filtered, and evaporated to dryness, giving a pale yellow oil. After purification by silica gel column chromatography (10% ethyl acetate/ 95% hexanes), the desired product was obtained as a light yellow oil (1.7 g, 61%). ¹H NMR (CDCl₃, 500 MHz): δ 11.37 (s, 2H, -CHO), 9.91 (s, 2H, -OH), 7.62 (s, 2H), 7.56 (d, *J* = 7.5 Hz, 2H), 7.48–7.41 (m, 6H), 7.35 (d, *J* = 1.5 Hz, 2H), 4.69 (s, 4H), 2.39 (s, 6H) ppm. ¹³C NMR (CDCl₃, 125 MHz): δ 197.06, 157.84, 139.13, 138.55, 136.01, 133.25, 130.25, 129.39, 128.89, 128.88, 128.60, 127.31, 120.03, 72.38, 20.55 ppm. ESI-MS(-) = 465.3 [M-H]⁻ (Calcd = 465.2 [M-H]⁻).

[⁵⁷Fe₂(Mes)₄]. A small-scale synthesis of 57-iron enriched [Fe₄(Mes)₄] was undertaken using a procedure adapted from literature reports.²⁻⁴ 57-Iron metal (200 mg, 3.51 mmol, 95% enriched) was suspended in 4.0 mL of concentrated aqueous hydrochloric acid. The mixture was heated to 90 °C for ~4 h using no stir bar, which led to dissolution of the iron metal and eventual formation of a clear brown solution. The reaction is not complete if the solution is a yellow color; further air oxidation is required to convert iron(II) chloride to iron(III) chloride. Once the reaction is complete, aqueous HCl was removed in vacuo to give a pale yellow solid. The solid was transferred to a 10 mL Schlenk flask under a nitrogen atmosphere and treated with 3 mL of freshly distilled thionyl chloride to dehydrate the iron(III) chloride. The mixture was heated at 80 °C for 30 min until the solid became a black color. Excess thionyl chloride was removed by pumping on the black solid under vacuum for 3 h. About 10 mL of dry chlorobenzene was added to the reaction flask and the slurry was refluxed for 30 min to give a brown suspension, which indicates conversion of anhydrous iron(III) chloride to iron(II) chloride. The septum-sealed reaction flask was brought inside an anaerobic glovebox for subsequent manipulations. The tan-colored solid was isolated by filtration and washed with toluene. This material was re-suspended in 3 mL of dry THF and stirred for 30

min until the brown solution became a beige color. An off-white solid was isolated by filtration as the desired $^{57}\text{FeCl}_2(\text{THF})_{1.5}$ precursor (571 mg, 53%).³

Inside an anaerobic drybox, a mesitylene Grignard reagent was prepared by combining 2-bromomesitylene (1.02 g, 5.12 mmol) and magnesium metal (123 mg, 5.12 mmol) in 2 mL of dry THF. After ~ 5 h, most of the magnesium had dissolved and the solution became a pale light brown color. The Grignard reagent was placed inside a -30 °C freezer and allowed to cool. In a separate vial, solid $^{57}\text{FeCl}_2(\text{THF})_{1.5}$ (571 mg, 2.14 mmol) was suspended in 3 mL of tetrahydrofuran /1,4-dioxane (1:1) that has been cooled to -30 °C. The cold Grignard reagent was added over a 5 min period to the iron solution. The reaction mixture was stirred and allowed to warm slowly to RT. As the reaction progressed, the light brown slurry became a red color. After 2 h, a solid precipitate was removed by filtration and the filtrate was evaporated to dryness. The dried residue was extracted into diethyl ether, filtered, and placed inside a -30 °C freezer to crystallize over the course of ~14 h. A large amount of red crystalline material was isolated by filtration and dried to give [$^{57}\text{Fe}_2(\text{Mes})_4$] as a red powder (430 mg, 60%). The spectroscopic characteristics of this compound are identical to those reported for [$\text{Fe}_2(\text{Mes})_4$].⁴ This product was stored at -30 °C inside the glovebox to prevent oxidation and thermal degradation.

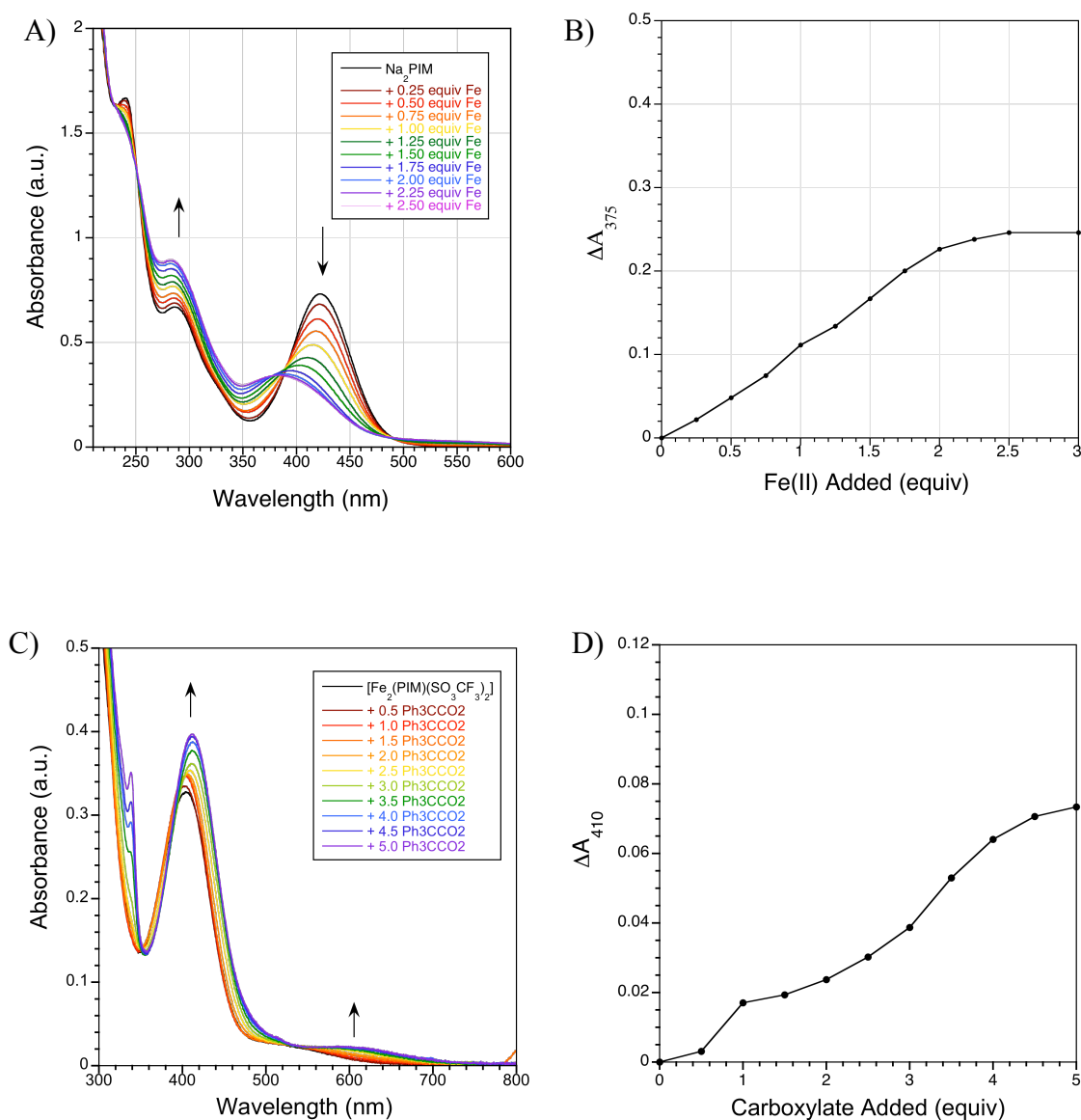


Figure S1. Optical changes upon addition of $\text{Fe}(\text{SO}_3\text{CF}_3)_2(\text{CH}_3\text{CN})_2$ to a $24 \mu\text{M}$ solution of PIM^{2-} in THF (panel A). Absorbance change at 375 nm clearly shows a 1:2 macrocycle to ligand binding stoichiometry (panel B). Addition of sodium triphenylacetate to a THF solution containing $\text{PIM}^{2-}/2 \text{ Fe}(\text{SO}_3\text{CF}_3)_2(\text{CH}_3\text{CN})_2$ led to absorption increases at ~ 410 and 600 nm (panel C). The single wavelength plot at 410 nm (D).

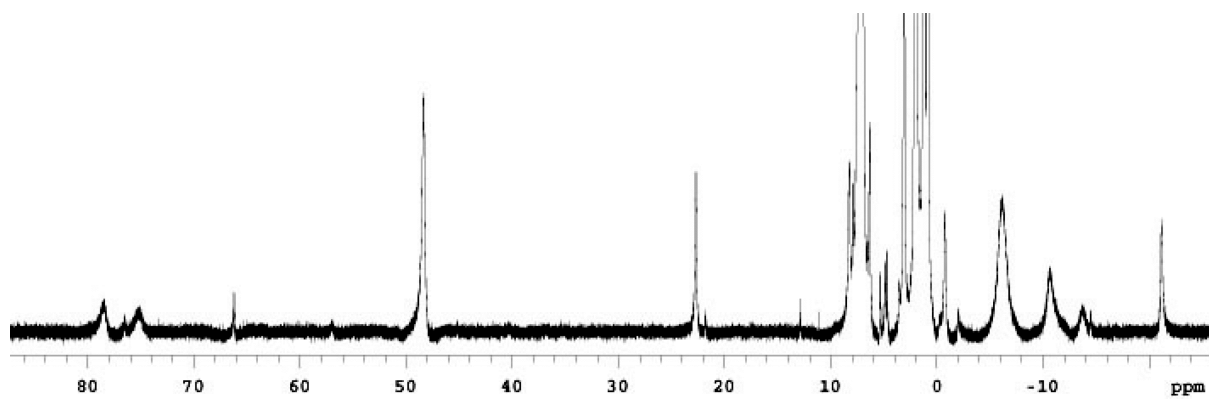


Figure S2. ¹H NMR spectrum (500 MHz) of a 5.0 mM solution of [Fe₂(PIM)(Ph₃CCO₂)₂] (**1**) in CD₂Cl₂ at room temperature.

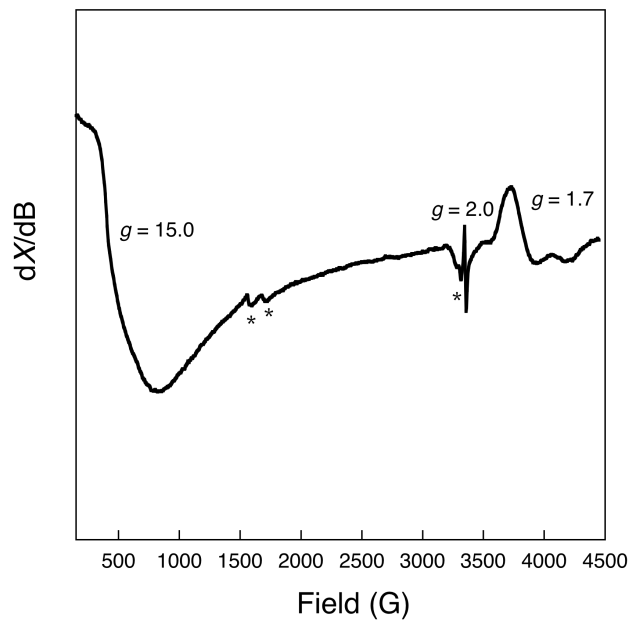


Figure S3. EPR spectrum of a frozen solution of $[\text{Fe}_2(\text{PIM})(\text{Ph}_3\text{CCO}_2)]$ (**1**) in 2-methyltetrahydrofuran measured at 5 K. The peaks marked with an asterisk are due to contaminants from the instrument cavity. The features centered at $g \approx 1.7$ is of unknown origin. Instrument parameters: 9.281 GHz microwave frequency; 2.002 mW microwave power; 1.00×10^4 receiver gain; 100.0 kHz modulation frequency; 2.00 G modulation amplitude; 2.560 ms time constant.

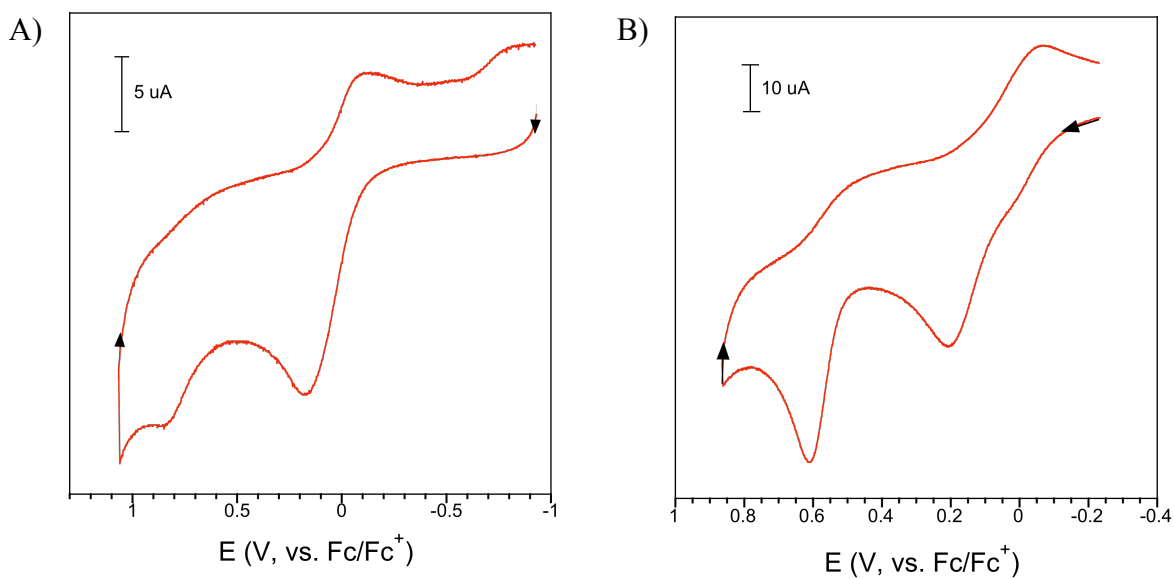


Figure S4. Cyclic voltammograms of 1.0 mM solutions of **1** (panel A) and **2** (panel B) in dichloromethane at a scan rate of 500 mV/s. Tetra-*n*-butylammonium hexafluorophosphate (0.2 M) was used as the supporting electrolyte. All data were obtained using a platinum working electrode and the electrochemical potentials were referenced externally to ferrocene/ferrocenium.

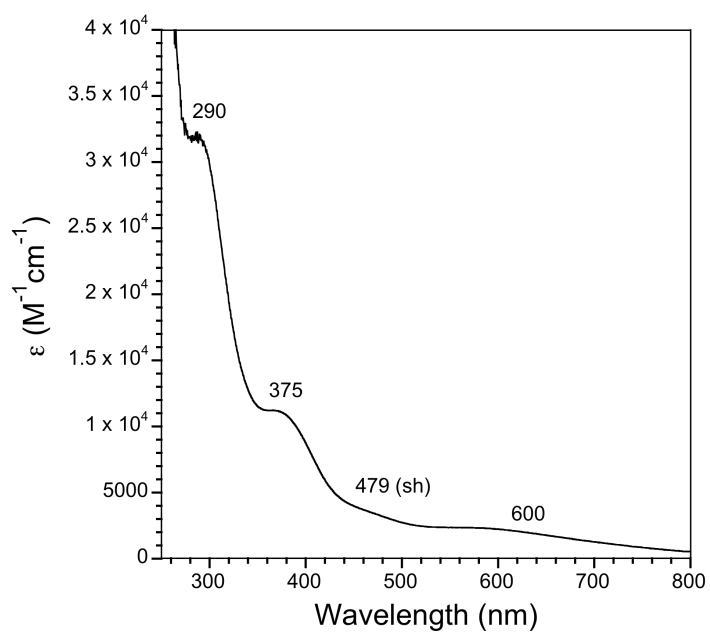


Figure S5. Absorption spectrum of $[Fe_2(\mu-OH)_2(ClO_4)_2(PIM)(\mu-Ar^{Tol}CO_2)Ag]$ (**3**) in dichloromethane

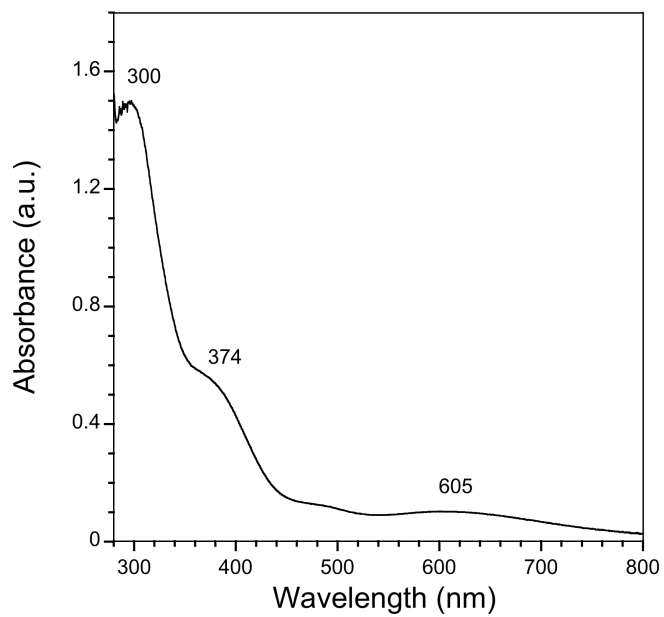


Figure S6. Absorption spectrum of the soluble product obtained from reaction of **2** with AgSbF_6 . The data were recorded in dichloromethane at a concentration of $\sim 40 \mu\text{M}$.

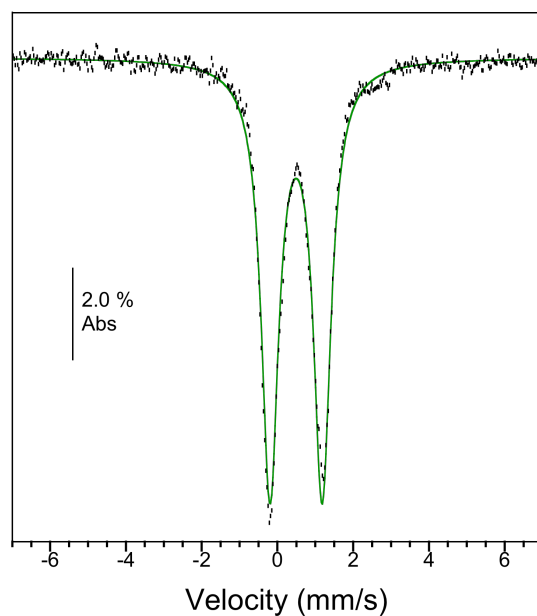


Figure S7. Zero-field Mössbauer spectrum (80 K) of a $[\text{}^{57}\text{Fe}_2(\text{OH})_2(\text{ClO}_4)_2(\text{PIM})(\text{Ar}^{\text{Tol}}\text{CO}_2)\text{Ag}]$ (**3**) solution in tetrahydrofuran. The data were fit to a single quadrupole doublet with $\delta = 0.49(2)$ mm/s, $\Delta E_Q = 1.38(2)$ mm/s, and $\Gamma = 0.56(2)$ mm/s. Raw data are shown in black and the spectral fit is shown in green.

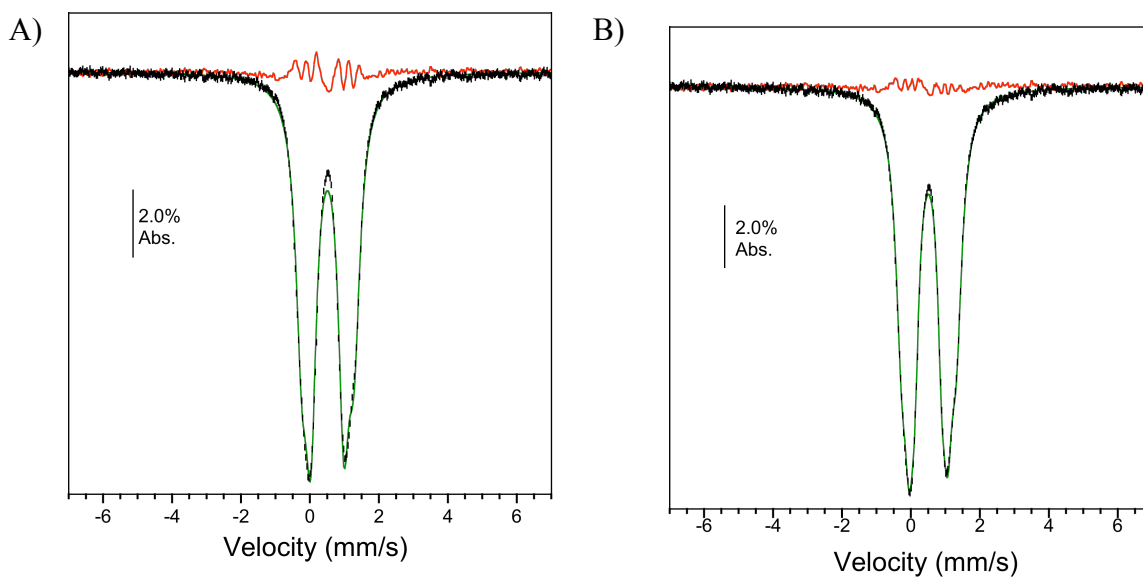


Figure S8. Zero-field Mössbauer spectrum (80K) of a frozen benzene- d_6 solution of $[\text{}^{57}\text{Fe}_2(\text{PIM})(\text{Ph}_3\text{CCO}_2)_2]$ ($^{57}\text{Fe-1}$)/ O_2 (black lines). The ^1H NMR spectrum of this sample is shown in Figure 9A. Spectral simulations are represented in green and fit residuals in red. Both plots show the same data, but are overlaid with different spectral fits for comparing their overall goodness of fit. Spectrum A was fit to a two-site model, with $\delta_1 = 0.50(2)$ mm/s, $\Delta E_{Q1} = 0.95(2)$ mm/s, $\Gamma_1 = 0.39(2)$ mm/s, Area 1 = 54%, $\delta_2 = 0.52(2)$ mm/s, $\Delta E_{Q2} = 1.52(2)$ mm/s, $\Gamma_2 = 0.44(2)$ mm/s, and Area 2 = 46%. Spectrum B was fit to a three-site model, with $\delta_1 = 0.50(2)$ mm/s, $\Delta E_{Q1} = 0.78(2)$ mm/s, $\Gamma_1 = 0.30(2)$ mm/s, Area 1 = 24%, $\delta_2 = 0.51(2)$ mm/s, $\Delta E_{Q2} = 1.12(2)$ mm/s, $\Gamma_2 = 0.34(2)$ mm/s, Area 2 = 37%, $\delta_3 = 0.52(2)$ mm/s, $\Delta E_{Q3} = 1.59(2)$ mm/s, $\Gamma_3 = 0.41(2)$ mm/s, and Area 3 = 39%. Comparing the fit residuals between A and B clearly demonstrate that the three-site model in B is a better representation of the data.

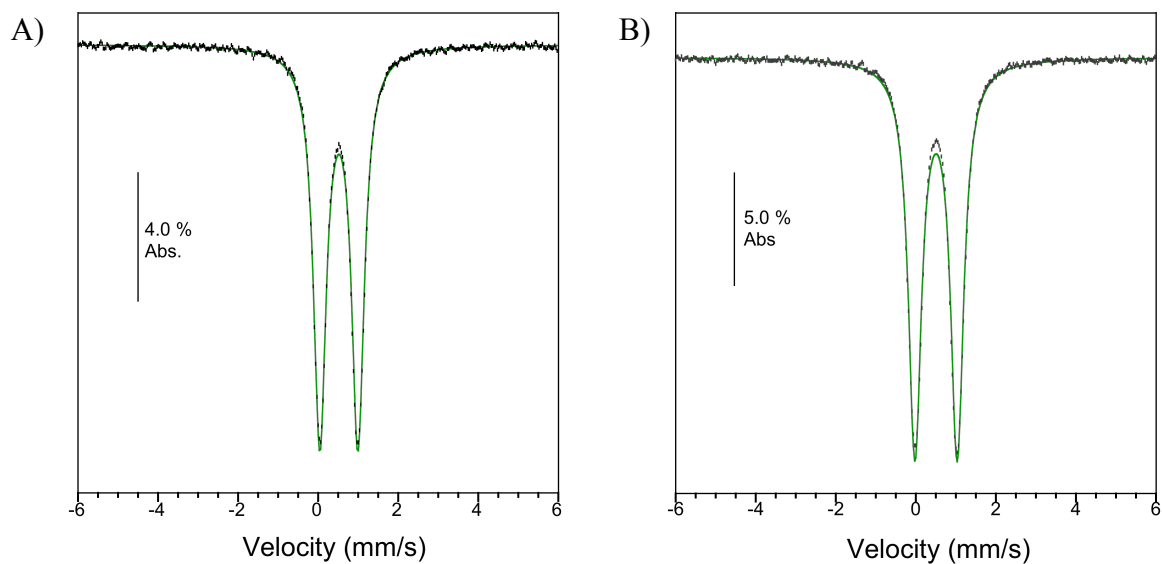


Figure S9. Zero-field Mössbauer spectrum (80 K) of polycrystalline samples of $[\text{}^{57}\text{Fe}_2(\text{OH})(\text{PIM})(\text{Ph}_3\text{CCO}_2)_3]$ (**4**, left) and $[\text{}^{57}\text{Fe}_4(\text{OH})_6(\text{PIM})_2(\text{Ph}_3\text{CCO}_2)_2]$ (**5**, right). Spectrum A gave Mössbauer parameters $\delta = 0.52(2)$ mm/s, $\Delta E_Q = 0.95(2)$ mm/s, and $\Gamma = 0.38(2)$ mm/s, whereas spectrum B returned Mössbauer parameters $\delta = 0.51(2)$ mm/s, $\Delta E_Q = 1.06(2)$ mm/s, and $\Gamma = 0.40(2)$ mm/s. Raw data are shown in black and the spectral fits are shown in green.

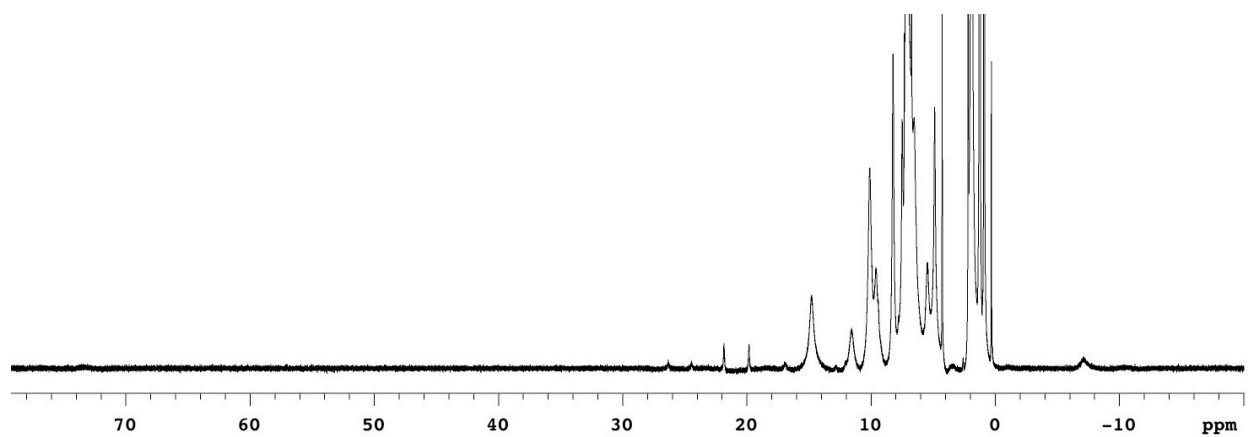


Figure S10. ¹H NMR spectrum (CD₂Cl₂, 500 MHz) of [Fe₂(PIM)(Ar^{Tol}CO₂)₂] (**2**) after exposure to dioxygen. The spectrum was recorded at room temperature at a diiron complex concentration of ~5.0 mM.

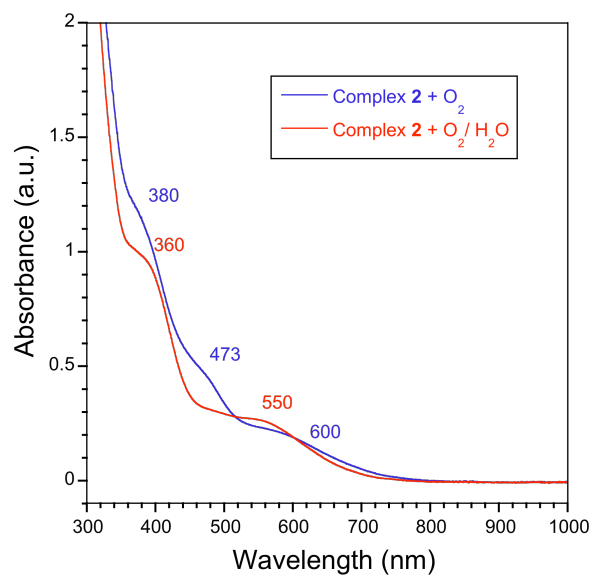


Figure S11. Absorption spectra of A) complex **2** + O₂ and B) complex **2** + O₂/ H₂O in dichloromethane. Spectrum A arises from a mixture of [Fe₂(μ-O)(PIM)(Ar^{Tol}CO₂)₂] (**6**) and [Fe₂(μ-OH)₂(PIM)(Ar^{Tol}CO₂)₂] (**7**) species. Spectrum B is assigned to a tetranuclear [Fe₄(μ-OH)₆(PIM)₂(Ar^{Tol}CO₂)₂] (**8**) complex.

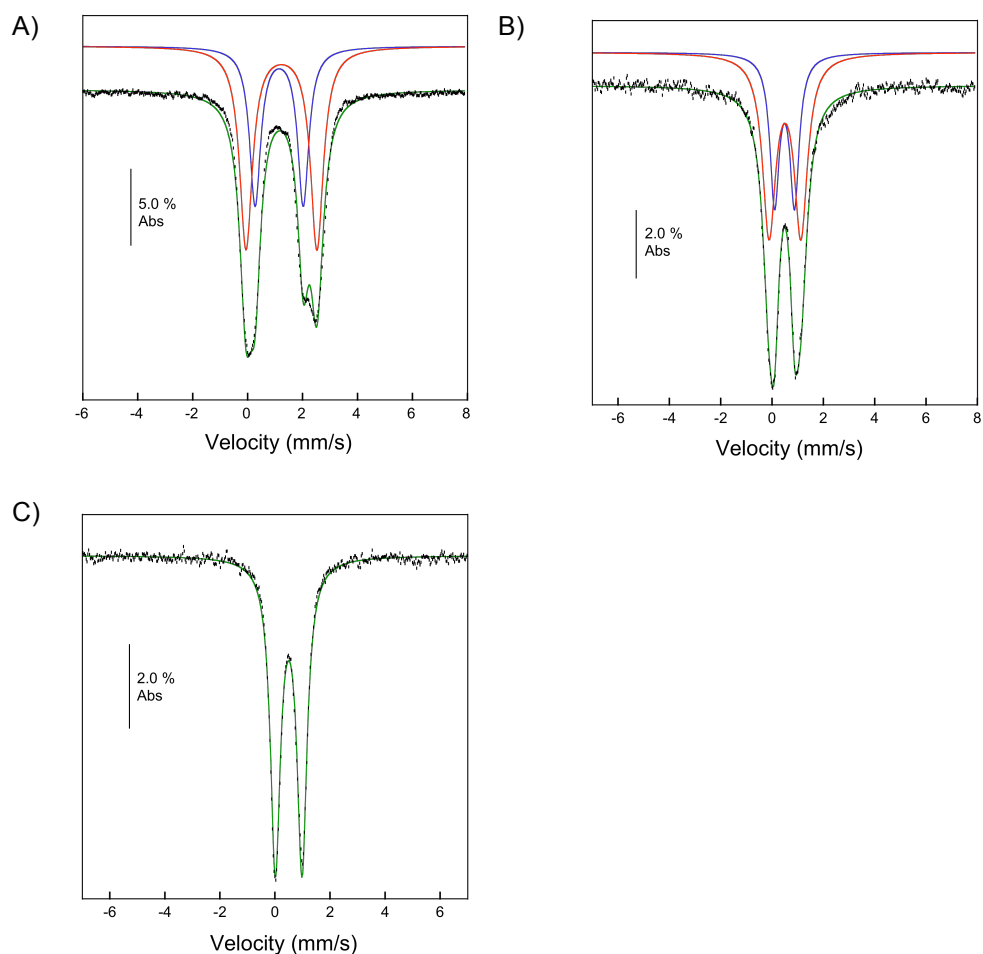


Figure S12. Zero-field Mössbauer spectra (80K) of a 22 mM $[^{57}\text{Fe}_2(\text{PIM})(\text{Ar}^{13\text{C}18}\text{CO}_2)_2]$ (**2**) solution in tetrahydrofuran (A) that was frozen after exposure to dioxygen (B) or dioxygen/ water (C). Spectrum A was best fit to a two-site model, which is consistent with the two different iron environments in **2**. The spectrum in B is assigned to two diiron species **6** and **7**, whereas the spectrum in C is assigned to a tetranuclear complex **8** containing equivalent iron sites. See Table 1 for solution Mössbauer parameters for species **2**, **6/7**, and **8**. Raw data are represented in black; spectral fits are shown in green, with unique iron sites displayed as either red or blue lines.

X-ray Crystallographic Refinement

X-ray diffraction quality crystals were selected out of the crystallization vials and immediately immersed in degassed Partone oil to prevent solvent loss and reaction with air. Complex **1** contains both benzene and pentane molecules in the asymmetric unit. Three of the benzene molecules were refined with full occupancy, whereas one of the benzene rings was substitutionally disordered with pentane. The benzene-to-pentane ratio refined to 55:45. The structure of **2** shows significant thermal motion within the tolyl groups of the terphenylcarboxylate ligands in the solid state, as indicated by the larger anisotropic displacement parameters of their carbon atoms compared to those of the rest of the molecule. Several solvent molecules were located in the crystal structure of **2**. In each asymmetric unit there are 1.39 pentane and 0.45 dichloromethane molecules. A pentane that is located on an inversion center shares partial occupancy with a pentane that does not lie on a special position. Another pentane molecule shares partial occupancy with dichloromethane, with a pentane/dichloromethane ratio of 39:45. The silver atom in **3** occupies two positions and is coordinated to O(5) of a bridging hydroxide, O(6) of the PIM²⁻ ligand, and an arene ring of the terphenylcarboxylate ligand. Because the H atoms of the bridging hydroxo groups in **3** could not be located from a difference electron density map, the hydrogen atoms attached to O(6) and O(7) were not included in the structure refinement. Four dichloromethane molecules per diiron complex occur in the structure of **3**, three of which have full occupancy whereas one is disordered. Complex **4** was unambiguously assigned as a (μ -hydroxo)diiron species because electron density corresponding to the hydrogen atom of O(6) was located from the difference electron density map. The asymmetric unit of **4** also contains two fully occupied ordered and one disordered benzene molecule. The center of the tetranuclear complex **5** lies on an inversion center; thus, there is only half a molecule in the asymmetric unit. There are four benzene molecules in the asymmetric unit. The structure of **6/7** clearly shows two different diiron cores, one containing a single bridging oxygen atom and another con-

taining two bridging oxygen atoms. The occupancy of the one vs. two oxygen bridges was refined to be 76% to 24%, respectively. Each $\frac{6}{7}$ unit also contains two fully occupied and one disordered acetonitrile solvent molecules. Complete X-ray data refinement parameters for complexes **1-7** are shown in Table S1.

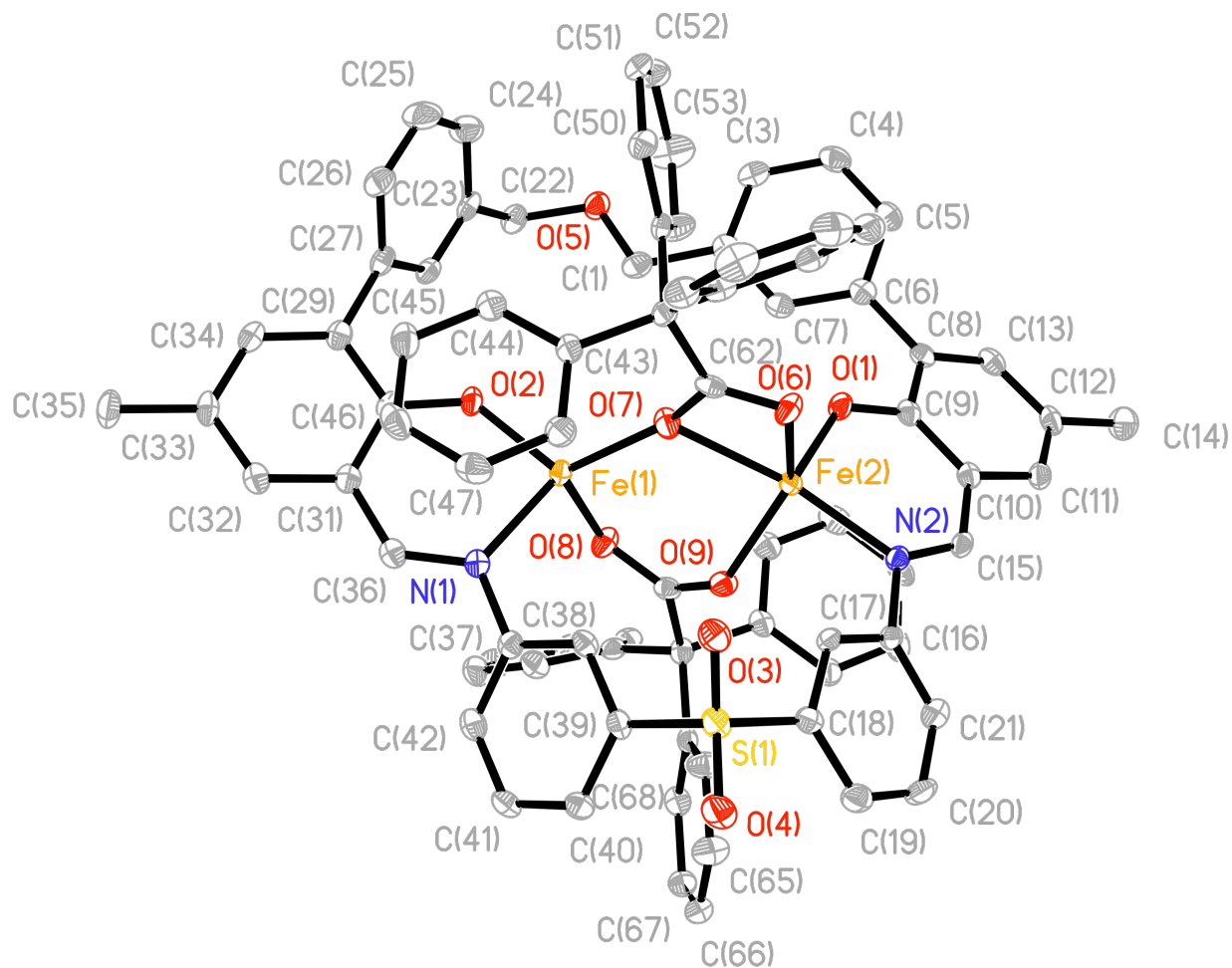


Figure S13. X-ray crystal structure of [Fe₂(PIM)(Ph₃CCO₂)₂] (1) shown with 50% thermal ellipsoids and a partial atom numbering scheme. Solvent molecules and hydrogen atoms have been omitted for clarity. Color representation: iron, orange; carbon, gray; oxygen, red; nitrogen, blue; sulfur, yellow.

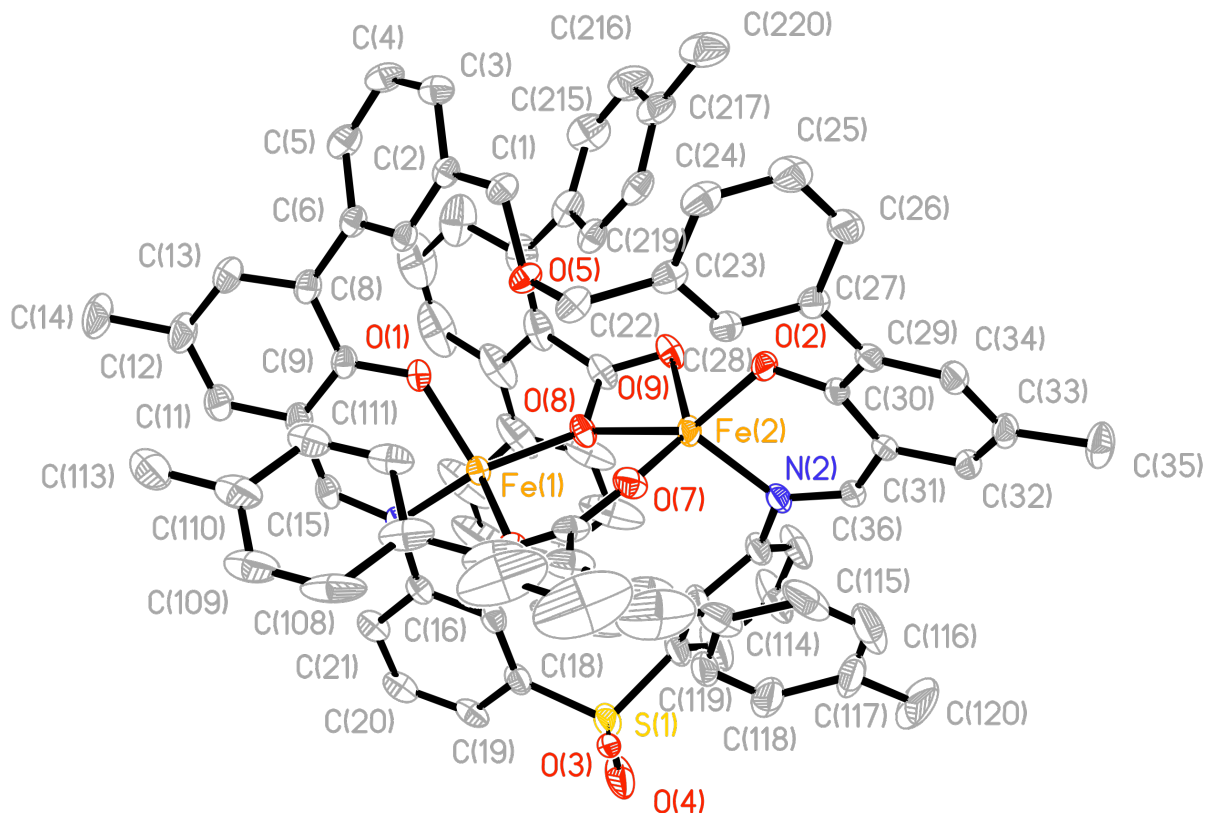


Figure S14. X-ray crystal structure of [Fe₂(PIM)(Ar^{Tol}CO₂)₂] (**2**) shown with 35% thermal ellipsoids and a partial atom numbering scheme. Solvent molecules and hydrogen atoms have been omitted for clarity. Color representation: iron, orange; carbon, gray; oxygen, red; nitrogen, blue; sulfur, yellow.

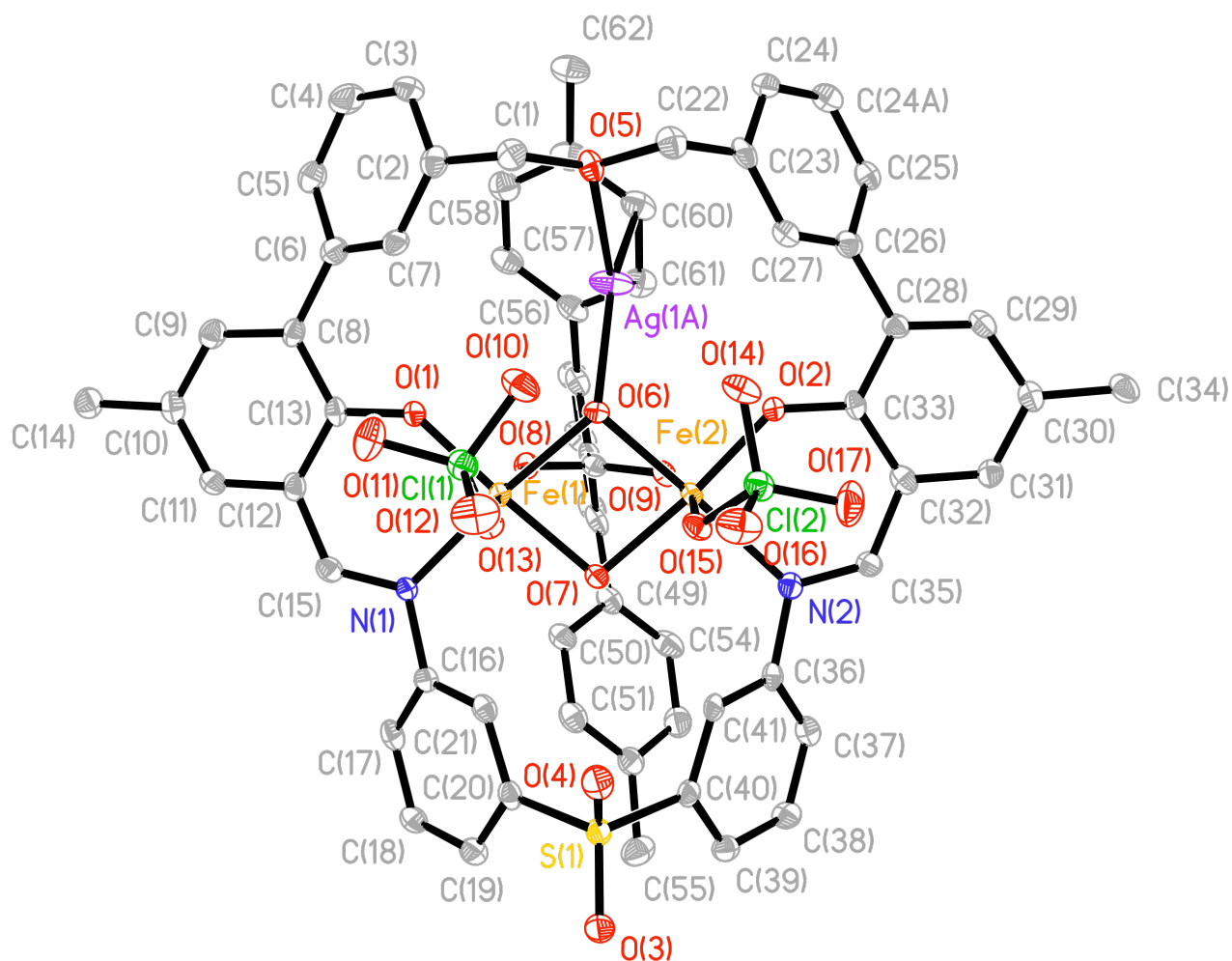


Figure S15. X-ray crystal structure of $[\text{Fe}_2(\mu\text{-OH})_2(\text{ClO}_4)_2(\text{PIM})(\text{Ar}^{\text{Tol}}\text{CO}_2)\text{Ag}]$ (**3**) shown with 50% thermal ellipsoids and a partial atom numbering scheme. Solvent molecules and hydrogen atoms have been omitted for clarity. Color representation: iron, orange; carbon, gray; oxygen, red; nitrogen, blue; sulfur, yellow; chlorine, green; silver, purple.

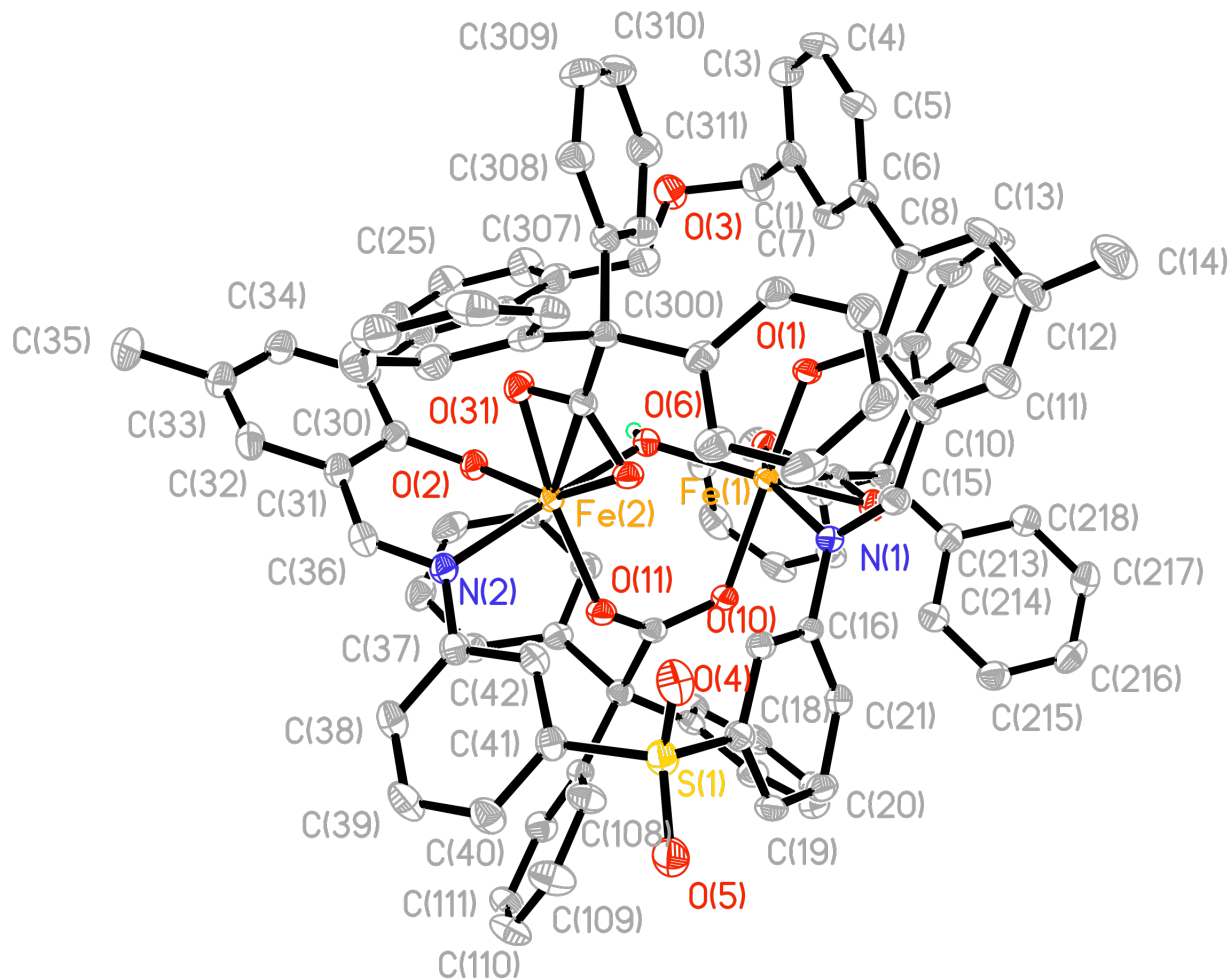


Figure S16. X-ray crystal structure of $[\text{Fe}_2(\mu\text{-OH})(\text{PIM})(\text{Ph}_3\text{CCO}_2)_3]$ (**4**) shown with 50% thermal ellipsoids and a partial atom numbering scheme. Solvent molecules and hydrogen atoms, except for the one attached to O(6), have been omitted for clarity. Color representation: iron, orange; carbon, gray; oxygen, red; nitrogen, blue; sulfur, yellow; hydrogen, green.

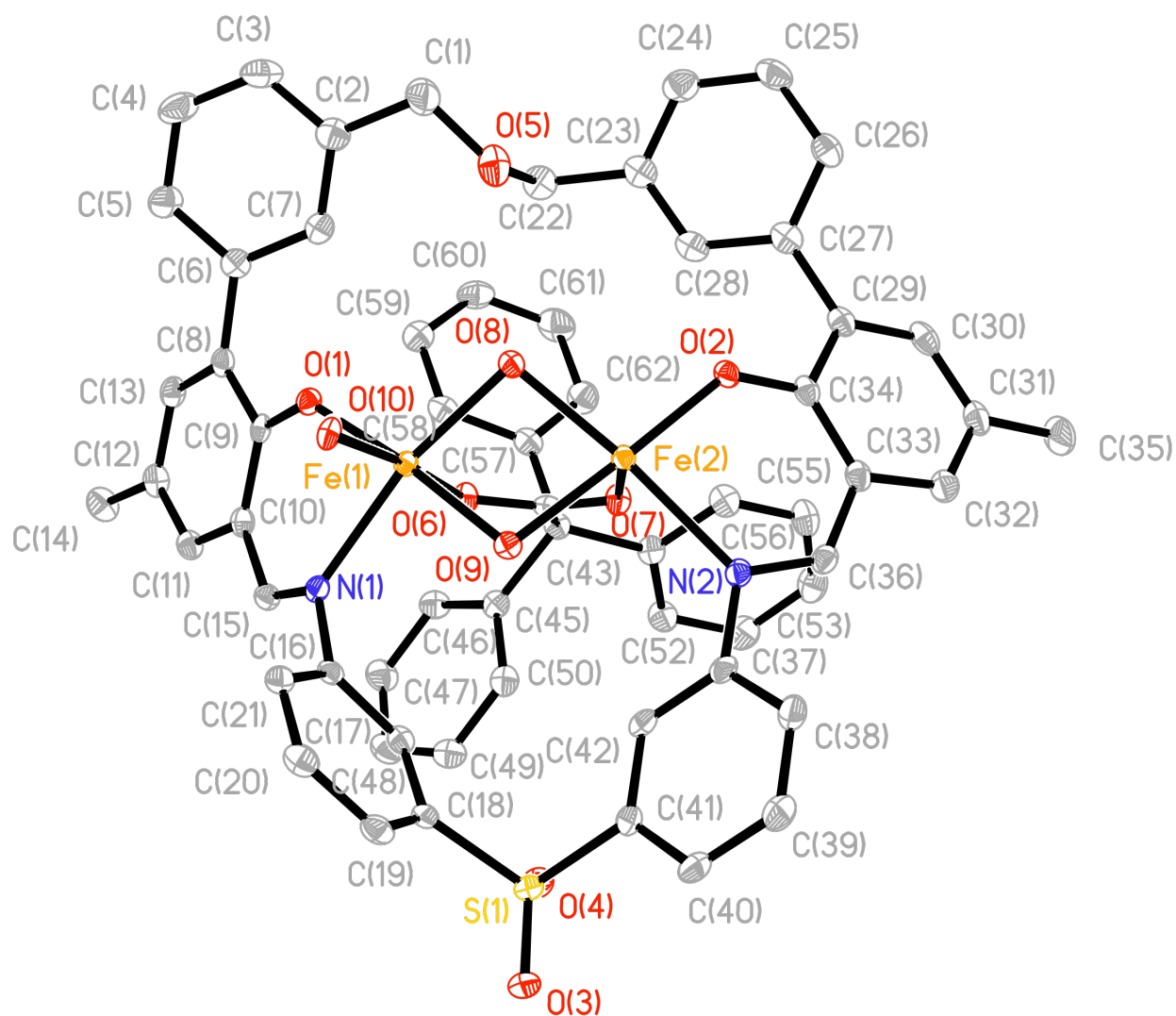


Figure S17. X-ray crystal structure of $[\text{Fe}_4(\mu\text{-OH})_6(\text{PIM})(\text{Ar}^{\text{Tol}}\text{CO}_2)_4]$ (**5**) shown with 50% thermal ellipsoids and a partial atom numbering scheme. Only half of the complex is depicted because the center of the molecule is located on an inversion center. Solvent molecules and hydrogen atoms have been omitted for clarity. Color representation: iron, orange; carbon, gray; oxygen, red; nitrogen, blue; sulfur, yellow.

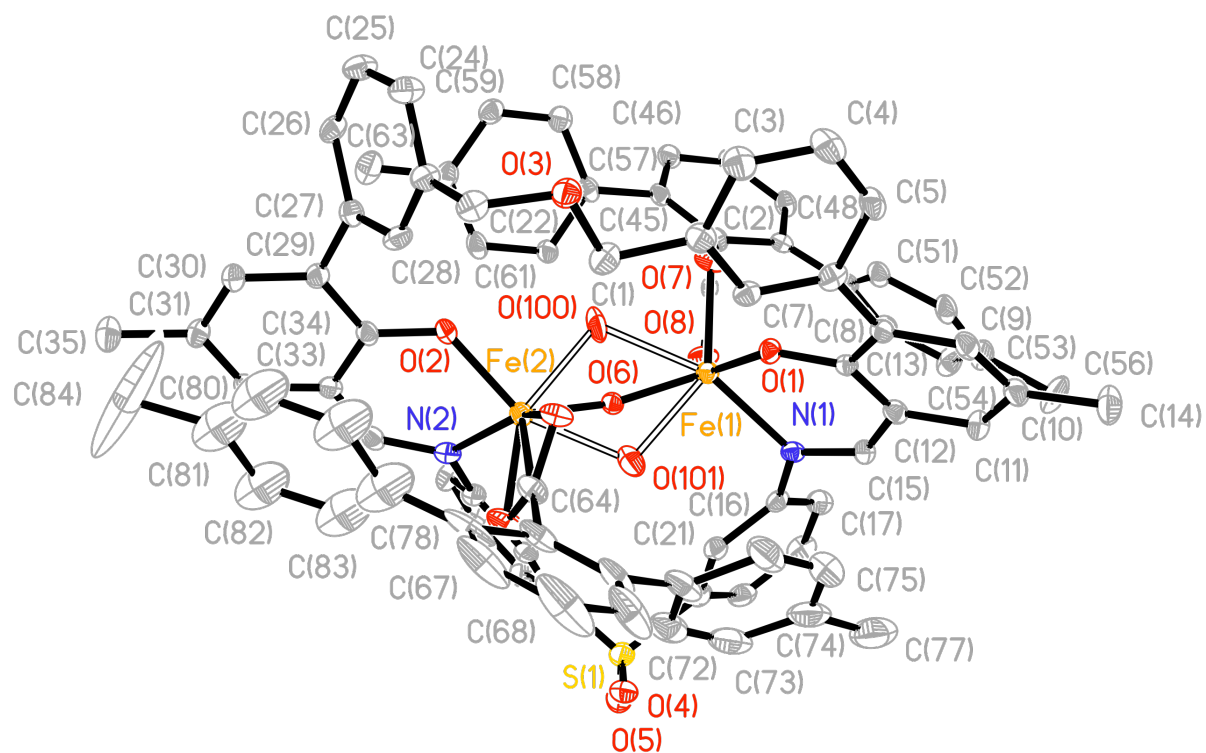


Figure S18. X-ray crystal structure of $[\text{Fe}_2(\mu\text{-O})(\text{PIM})(\text{Ar}^{\text{Tol}}\text{CO}_2)_2]$ (**6**) and $[\text{Fe}_2(\mu\text{-OH})_2(\text{PIM})(\text{Ar}^{\text{Tol}}\text{CO}_2)_2]$ (**M7**) shown with 35% thermal ellipsoids and a partial atom numbering scheme. The two oxygen atoms that comprises **M6** [O(100) and O(101)] and the one oxygen atom that comprises **M7** [O(6)] were refined as a positional disorder with occupancies of 76% and 24%, respectively. Solvent molecules and hydrogen atoms have been omitted for clarity. Color representation: iron, orange; carbon, gray; oxygen, red; nitrogen, blue; sulfur, yellow.